IOPscience iopscience.iop.org

Home Search Collections Journals About Contact us My IOPscience

Classical paths for the periodic potential

This article has been downloaded from IOPscience. Please scroll down to see the full text article.

1988 J. Phys. A: Math. Gen. 21 2351

(http://iopscience.iop.org/0305-4470/21/10/014)

View the table of contents for this issue, or go to the journal homepage for more

Download details:
IP Address: 129.252.86.83
The article was downloaded on 31/05/2010 at 13:24

Please note that terms and conditions apply.

J. Phys. A: Math. Gen. **21** (1988) 2351-2374. Printed in the UK

Classical paths for the periodic potential

D A Nicole† and P J Walters‡

† Department of Electronics and Computer Science, University of Southampton, Southampton SO9 5NH, UK

‡ Department of Adult Education, University College of Swansea, Singleton Park, Swansea SA2 8PP, UK

Received 15 June 1987, in final form 10 February 1988

Abstract. The classical path method is used to derive the WKB energy levels and wavefunctions for the periodic potential. The method generalises the instanton approach and can accommodate excited-state energy bands in addition to the ground-state band.

1. Introduction

The semiclassical approach to quantum mechanics becomes appropriate when the classical action is large compared with Planck's constant [1]. The natural way to express this is in terms of the Feynman path integral [2, 3]. The semiclassical approximation is the path integral evaluated considering only Gaussian fluctuations about the classical path. The WKB method also includes certain non-Gaussian fluctuations [4].

The WKB or semiclassical approximations are particularly useful in situations where quantum mechanical tunnelling is important. Barrier penetration is a phenomenon of fixed energy and thus we look at the energy Green function rather than the fixed time Feynman propagator. Tunnelling presents a problem for the path integral approach; the classical solutions to Newton's equations in the tunnelling regime require the use of imaginary time [5]. The classical path method has recently been developed [4] and treats all the solutions of Newton's equations in complex time in a unified way. The difficulty of solving problems in the classical path approach (or any other semiclassical method) is related to the topological complication of the classical paths. The linear potential, the quadratic potential well and barrier, together with the quartic double-well potential, were treated in the original paper on classical paths by Carlitz and Nicole [4]. More complicated potentials arising in the spontaneous breakdown of supersymmetric quantum mechanics were considered by Carlitz [6]. In this paper we treat the problem of the periodic potential, specifically the pendulum potential. Any periodically repeated bounded potential will have the same classical path structure and consequently the solution will have exactly the same form as that for the pendulum potential presented in this paper. However, we choose to specialise in the pendulum potential, because the solutions can be written explicitly and the action integrals evaluated exactly.

The pendulum potential is important because it is the simplest example (apart from the free rotor) which has significant topological complications. Thus classical solutions for the pendulum which just swings back and forth cannot be continuously deformed into solutions which have tunnelled around the centre of rotation with the same start

0305-4470/88/102351+24$02.50 © 1988 IOP Publishing Ltd

and end points. Therefore, the classical solutions fall into distinct classes identified by the winding number, which is the net number of 'rotations' about the centre. Similar, but generally more complicated examples, requiring homotopy theory for their classification, occur in field theory [7]. It is important to have a clear foundation in quantum mechanics before being satisfied with the generalisation in field theory.

In tackling this problem we will generally look on it as an 'electron' in an infinite periodic lattice, rather than a pendulum whose motion is restricted to a circle. Successive winding numbers for the pendulum now correspond to the particle tunnelling to adjacent lattice sites. The two problems are different but the solutions are closely related. Each energy level for the pendulum is spread out into a band in the problem of the infinite lattice.

The bound-state energies and wavefunctions obtained by the classical path method will be exactly the same as the WKB approximation to the solution of the Schrödinger equation. This problem has also been treated by Millard [8], although our approach is different. She gives a solution valid over a wider energy range, whereas we concentrate on understanding the detailed structure of the problem within the classical path method. The advantage of the classical path method lies in its convenience of application to complicated, and particularly multi-dimensional, problems. In this regard it is compared with the instanton approach which it generalises [4, 7].

Fröman [9, 10] has developed a phase integral formula which has some advantages over the WKB approximation. This is particularly evident in circumventing the connection problems and the associated Stokes discontinuities which arise in the WKB approach. The classical path method is a version of the WKB approximation and retains the Stokes discontinuities. However, we deal with the connection problems in a more efficient manner than the conventional approach. This method makes the origin and nature of the asymptotic expansion and its Stokes jumps clear.

The paper is organised as follows: in the next section we review the steepest descent approximation for the energy Green function, which lies at the heart of the classical path method. In § 3 we describe the classical paths for the pendulum and evaluate the WKB action for these paths. In § 4 we evaluate the semiclassical bound-state energies without considering the exponentially small tunnelling terms. The complication of the periodic potential problem arises from classifying the contributions from all the multiple tunnelling terms. How this is achieved, together with the evaluation of the sum over paths, is outlined in § 5. As previously mentioned, these results are valid for any simple periodic potential. The band energies obtained agree with those previously achieved by direct approximation of the Schrödinger equation. These results are compared with the tight binding approximation and the instanton approach.

2. Review of the classical path method

The starting point for the classical path method is the semiclassical approximation to the Feynman propagator [2] in one space dimension,

$$K(\phi_f, \phi_i; T) = \sum_{\substack{\text{classical} \\ \text{paths } \phi_{cl}}} \left(\frac{D}{2\pi i\hbar}\right)^{1/2} \exp\{iS_{cl}(\phi_f, \phi_i; T)/\hbar\} \tag{2.1}$$

where ϕ_{cl} is a classical path from ϕ_i to ϕ_f in time T and S_{cl} is the corresponding classical action. The factor D arising from the Gaussian integrals also has a classical

interpretation [2]. If we imagine all the classical paths emerging from ϕ_i, each classified by its energy, then the factor D can be interpreted as the density of these classical paths at the final position ϕ_f. Explicitly, D is given by the expressions [2, 11]

$$D = -\frac{\partial^2 S_{cl}}{\partial \phi_i \partial \phi_f} = -\frac{\partial E_{cl}/\partial T}{\dot{\phi}_{cl}(0)\dot{\phi}_{cl}(T)}. \tag{2.2}$$

The Gaussian approximation for K becomes inadequate near 'focal points'—where the density of classical paths D becomes singular. Thus it is important to observe that in Carlitz and Nicole [4] the singularities of K are found to make no contribution to the energy Green function G and thus their exact treatment is not required even though the contours in the complex T plane used to evaluate G pass through these singularities.

Classical turning points typically are not focal points as the zeros of $\dot{\phi}_{cl}$ are cancelled by a zero of $\partial E_{cl}/\partial T$. Classical turning points do require careful treatment of non-Gaussian fluctuations in the derivation of the G from K. $K(\phi_f, \phi_i; T)$ as given by (2.1) is an approximation to the exact kernel which can be defined as a functional integral.

The classical path method works with the energy Green function G, defined as the Laplace transform of the Feynman propagator:

$$G(\phi_f, \phi_i; E) = \frac{1}{i\hbar}\int_0^\infty dT \exp(iET/\hbar) K(\phi_f, \phi_i; T). \tag{2.3}$$

The idea underlying the method is based on work by McLaughlin [5]. He developed an analogy between the Feynman path integral for the kernel K and contour integral representations of special functions. Specifically, he demonstrated that it was possible to analytically continue the function space integral K with respect to the time parameter T. The integral (2.3) was then shown to be independent of the contour in complex time, provided the singularities of K were avoided. This allows the treatment of barrier penetration, whose classical solutions require imaginary time, within the path integral method. The approximation technique now depends upon selecting a suitable contour from which the asymptotic behaviour can be extracted. We note that the semiclassical approximation (2.1) retains the same form when the Gaussian integrals are evaluated along an arbitary path in complex time [5]. Hence, specialising in one particular classical path and substituting the semiclassical approximation, equation (2.3) becomes

$$G_{\phi_{cl}}(\phi_f, \phi_i; E) = \frac{1}{i\hbar}\int_0^\infty dT \left(\frac{D}{2\pi i\hbar}\right)^{1/2} \exp\{i(ET + S_{cl})/\hbar\}. \tag{2.4}$$

This integral is now evaluated by distorting the contour into complex time. Typically, the exponential term will oscillate producing cancellations, thus making a systematic approximation difficult. The steepest descent method chooses a contour to eliminate these unwelcome oscillations. There are some subtleties in this procedure and these will be explained shortly. However, it is clear that the main contribution to the integral occurs near the critical or saddle points, where the complex time derivative of the exponent vanishes. This gives the condition

$$E = -\partial S_{cl}/\partial T \equiv E_{cl}. \tag{2.5}$$

The saddle points T_s are the times for which a classical trajectory of energy E can pass from ϕ_i to ϕ_f. If the motion is periodic then there will be an infinite number of saddles T_s. In general, the Gaussian approximation for K becomes inadequate near 'focal points' where the density of classical paths D becomes singular. Let us consider

for clarity the simple example of the harmonic oscillator, described in Carlitz and Nicole [4]. Here, the action is given by

$$S=\frac{1}{2\lambda}\int_0^T \mathrm{d}t\{\dot{\phi}^2(t)-\omega^2\phi^2(t)\}. \tag{2.6a}$$

The Gaussian result for K is in fact exact, and given by

$$K(\phi_\mathrm{f},\phi_\mathrm{i};T)=\left(\frac{\omega}{2\pi\mathrm{i}\lambda\hbar\sin(\omega T)}\right)^{1/2}\exp\left(\frac{\mathrm{i}\omega[(\phi_\mathrm{i}^2+\phi_\mathrm{f}^2)\cos(\omega T)-2\phi_\mathrm{i}\phi_\mathrm{f}]}{2\lambda\hbar\sin(\omega T)}\right). \tag{2.6b}$$

The focal points in the complex-T plane are the singularities of K, given in our example by $\omega T=n\pi$. Paths of various energies setting off from ϕ_i at time $T=0$ reconverge after multiples of half a classical period. In this example the Gaussian approximation correctly reproduces genuine singularities of K. For more complex systems, the Gaussian approximation will predict singularities in K at each singularity of S_cl. These may not, however, be present in the exact K. They are typical of the spurious analytic behaviour exhibited by asymptotic approximations away from their range of validity.

Let us first consider the harmonic oscillator, where we have already established a sequence of focal points given by $\omega T=n\pi$. We choose the initial and final positions in the classically inaccessible region on opposite sides of the potential. This means that the saddle points, corresponding to classical paths, will move into the complex-time plane because of tunnelling. Now the real time elapsed must be $\mathrm{Re}(\omega T)=(2n+1)\pi$, i.e. the time to cross the allowed region plus any number of additional whole periods. Distorting the contour to pass through the saddles gives a picture very like that shown in figure 8 provided we identify $K=\frac{1}{2}\pi$ and $K'=\infty$. The path breaks up into an infinite number of separate saddle contributions. Generally, we will evaluate the integral (2.4) in a similar way. The contour is deformed so as to pass through saddles of S_cl following steepest descent trajectories which end at focal point singularities of S_cl. A typical path then falls into several separate saddle contributions as just described for the harmonic oscillator. Following the method of Dingle [12] we define a new variable f which measures distance along a saddle contribution: $f=\pm\infty$ at the terminal singularities and $f=0$ at the saddle. For a single saddle contribution

$$\frac{\mathrm{i}W_\mathrm{cl}(T)}{\hbar}\equiv\frac{\mathrm{i}}{\hbar}(ET+S_\mathrm{cl}(T))=\frac{\mathrm{i}}{\hbar}[ET_\mathrm{S}+S_\mathrm{cl}(T_\mathrm{S})]-f^2 \tag{2.7}$$

and f^2 can be expanded by Taylor series as

$$f^2=\frac{\mathrm{i}}{\hbar}\left(\left.\frac{\partial E}{\partial T}\right|_{T_\mathrm{S}}\frac{(T-T_\mathrm{S})^2}{2!}-\left.\frac{\partial^2 E}{\partial T^2}\right|_{T_\mathrm{S}}\frac{(T-T_\mathrm{S})^3}{3!}+\ldots\right). \tag{2.8}$$

In general the saddles T_S will be complex with the steepest descent contour defined by the condition

$$\mathrm{Im}\,f^2=0 \qquad \text{or} \qquad \mathrm{Re}\;W_\mathrm{cl}(T)=\mathrm{Re}\;W_\mathrm{cl}(T_\mathrm{s})=\text{constant}. \tag{2.9}$$

Recall that at focal points $\partial E/\partial T$ becomes infinite and so f becomes singular. There will be an infinite number of saddle points on a typical classical path $\phi_\mathrm{cl}(T)$ as the time increases to infinity. The Green function can now be written

$$G(\phi_\mathrm{f},\phi_\mathrm{i};E)=\sum_{\substack{\text{saddles on}\\ \text{classical path}}}\frac{\exp(\mathrm{i}W_\mathrm{cl}(T_\mathrm{s})/\hbar)}{\mathrm{i}\hbar}\left[\int_{-\infty}^{+\infty}\mathrm{d}f\left(\frac{\mathrm{d}T}{\mathrm{d}f}\right)\left(\frac{D}{2\pi\mathrm{i}\hbar}\right)^{1/2}\mathrm{e}^{-f^2}\right] \tag{2.10a}$$

with

$$\frac{\mathrm{d}T}{\mathrm{d}f}=\frac{2\mathrm{i}f}{\hbar(E+\partial S_{\mathrm{cl}}/\partial T)}. \tag{2.10b}$$

Not all the saddle points correspond to physical motions and some care must be taken in choosing which saddles to include in the summation. To see how this arises we express the elapsed time and WKB action W in terms of the energy and the complex path. Energy conservation gives the condition

$$E=\dot{\phi}^2/2\lambda+V(\phi) \tag{2.11}$$

where V is the potential. Thus we can write the time and WKB action as

$$T=\int_{\phi_{\mathrm{i}}}^{\phi_{\mathrm{f}}}\frac{\mathrm{d}\phi(t)}{[2\lambda(E-V(\phi))]^{1/2}} \tag{2.12a}$$

$$W=\int_{\phi_{\mathrm{i}}}^{\phi_{\mathrm{f}}}p_{\mathrm{cl}}(t)\,\mathrm{d}\phi(t)=\frac{1}{\lambda}\int_{\phi_{\mathrm{i}}}^{\phi_{\mathrm{f}}}[2\lambda(E-V(\phi))]^{1/2}\,\mathrm{d}\phi(t) \tag{2.12b}$$

where $p_{\mathrm{cl}}(t)$ is the classical momentum along the path ($p_{\mathrm{cl}}=\dot{\phi}/\lambda$). Notice that these expressions contain a square root branch point at turning points ($\dot{\phi}=0$ or $E=V$). In the simple case of the harmonic oscillator there are only two turning points. To make these expressions unambiguous we define the position, ϕ, on a suitable Riemann surface. However, we now have an ambiguity over which sheet the initial and final positions should be assigned. The physical positions are chosen by two criteria. First the physical motion moves forward and hence the real part of the time must be positive. The second criterion requires that tunnelling be suppressed and this demands that the imaginary part of the action W be positive. However, non-physical motions rejected by these conditions will still give rise to spurious saddle points.

To evaluate the integral (2.10a), $\sqrt{D}\ \mathrm{d}T/\mathrm{d}f$ is expanded as a Taylor series in f, giving a leading contribution

$$\frac{\mathrm{d}T}{\mathrm{d}f}\simeq\sqrt{2}\left(\frac{\mathrm{i}}{\hbar}\frac{\partial E}{\partial T}\bigg|_{T_{\mathrm{s}}}\right)^{-1/2}. \tag{2.13}$$

Notice from equation (2.10b) that $\mathrm{d}T/\mathrm{d}f$ becomes singular at the saddle point closest to the saddle at T_{s}. This saddle may be non-physical, but it nevertheless controls the radius of convergence of the Taylor series for $\sqrt{D}\ \mathrm{d}T/\mathrm{d}f$. This radius of convergence will be inside the infinite range of the Gaussian integration, which means that the series we obtain for the energy Green function will be an asymptotic rather than a convergent series [12]. This technical misdemeanour, of integrating a series term by term beyond its radius of convergence, is Dingle's [12] approach to generating asymptotic expansions. This technical error can be precisely reversed by the technique of (modified) Borel resummation. Despite its divergence, the first term in the asymptotic series will provide a good approximation when the singularities of $\mathrm{d}T/\mathrm{d}f$ occur for large f, as the Gaussian exponential will make the integral negligible well before the questionable region is reached. Thus if T_{s}' is the nearest saddle to the saddle point T_{s} we require

$$|W_{\mathrm{cl}}(T_{\mathrm{s}}')-W_{\mathrm{cl}}(T_{\mathrm{s}})|\gg\hbar. \tag{2.14}$$

When this condition is satisfied the first term in the asymptotic series provides a good approximation. Thus our basic formula for the energy Green function is

$$G(\phi_f, \phi_i; E) \simeq \sum_{\substack{\text{physical} \\ \text{saddles}}} \frac{\exp[i W_{cl}(T_s)/\hbar]}{\hbar[e^{i\pi}\dot{\phi}_i(0)\dot{\phi}_f(T_s)]^{1/2}}. \tag{2.15}$$

For condition (2.14) to be satisfied we require that the classical turning points be well separated from each other and from the initial and final positions. Thus the steepest descent approximation for the one-dimensional integral (2.3) breaks down when the turning points begin to coalesce (near the top and bottom of the potential well). However, the semiclassical approximation remains valid in these circumstances. (Recall that it becomes inadequate near focal points.) Thus the integral (2.3) may be evaluated by other conventional techniques.

Expression (2.15) represents a typical asymptotic approximation. The right-hand side has extra singularities, away from the domain of validity of the approximation, not contained in $G(\phi_f, \phi_i; E)$. Additionally, as ϕ_i, ϕ_f and E vary, the set of physical saddles jump on or off the physical contour. The resultant Stokes jumps in the approximation serve to repair the analytic behaviour of the approximation in its domain of validity.

Formulae (2.15) corresponds to the path integral version of the WKB approximation. It is valid when the classical turning points are well separated; in fact, it reproduces the WKB result for systems with isolated turning points. The classical path method is not limited to this case. When the turning points approach each other, the Laplace integral summing the contribution of all the relevant classical paths can be evaluated as shown by Carlitz and Nicole [4]. This allows the derivation of the WKB result with quadratic turning points and we will quote their results where relevant.

3. Classical paths for the pendulum

In order to put into effect the procedure for the classical path method outlined in the previous section, a number of preliminary quantities and properties must be established. We organise this section into subheadings with this in mind. We begin with the notation, equations of motion and basic solutions to the pendulum motion. The next subsection establishes the focal points of the motion. This is essential preparation for deforming the contour into complex time. Formulae (2.15) also requires that the WKB action be evaluated. The procedure for achieving this is outlined in § 3.3. Finally, the enormous variety of classical paths are classified in § 3.4. The various sums over physical paths required in formula (2.15) will then be carried out in §§ 4 and 5.

3.1. Notation

We take the Lagrangian for the simple pendulum as

$$L = \frac{1}{\lambda}[\tfrac{1}{2}\dot{\phi}^2 - \omega^2(1-\cos\phi)] = \frac{1}{\lambda}[\tfrac{1}{2}\dot{\phi}^2 - 2\omega^2 \sin^2(\tfrac{1}{2}\phi)] \tag{3.1}$$

where $\phi(t)$ is the angular displacement. The equation of motion is

$$\ddot{\phi}(t) = -\omega^2 \sin\phi. \tag{3.2}$$

The classical solution is given in terms of Jacobi elliptic functions with modulus k, by the equation

$$\sin(\tfrac{1}{2}\phi(t)) = k\,\mathrm{sn}(\omega t+\alpha;\,k) \tag{3.3a}$$

where k and α are variables of integration corresponding to amplitude and phase. The corresponding conjugate momentum is given by

$$p(t) = \dot{\phi}(t)/\lambda = (2k\omega/\lambda)\,\mathrm{cn}(\omega t+\alpha;\,k). \tag{3.3b}$$

3.2. Determination of the focal points

For small amplitude oscillations we know that the pendulum is approximated by the harmonic oscillator. For the harmonic oscillator the trajectories reconverge after multiples of a half period, as discussed in the previous section. For the pendulum motion the paths also cross every half period ($2K$ where K, the quarter period, will be defined shortly). However, unlike the harmonic oscillator the focusing is not perfect. These focal points are not true singularities of the propagator but just artefacts of the semiclassical method. Nevertheless the propagator will be large and in the classical path method this is all that is required. The elliptic functions are doubly periodic and so it is reasonable to predict that focal points will also occur in imaginary time at multiples of the imaginary half period (i.e. $2K'$). These results will now be established more explicitly.

In determining the classical action S_{cl} we require the classical path that moves from ϕ_{i} to ϕ_{f} in time T. This demands that the initial and final conditions are given by

$$\sin(\tfrac{1}{2}\phi_{\mathrm{i}}) = k\,\mathrm{sn}\,\alpha \tag{3.4a}$$

and

$$\begin{aligned}\sin(\tfrac{1}{2}\phi_{\mathrm{f}}) &= k\,\mathrm{sn}(\omega T+\alpha)\\ &= \frac{\mathrm{sn}(\omega T)(k\,\mathrm{cn}\,\alpha\,\mathrm{dn}\,\alpha)+\sin(\tfrac{1}{2}\phi_{\mathrm{i}})\,\mathrm{cn}(\omega T)\,\mathrm{dn}(\omega T)}{1-\sin^2(\phi_{\mathrm{i}}/2)\,\mathrm{sn}^2(\omega T)}.\end{aligned} \tag{3.4b}$$

We have dropped the explicit reference to the modulus k in the elliptic functions and substituted the initial condition (3.4a) into the expansion for the final condition. The classical solution incorporating conditions (3.4) can be expressed as

$$\begin{aligned}\sin(\tfrac{1}{2}\phi_{\mathrm{cl}}(t)) &= k\,\mathrm{sn}(\omega t+\alpha)\\ &= \frac{A(T)\,\mathrm{sn}(\omega t)+\sin(\tfrac{1}{2}\phi_{\mathrm{i}})\,\mathrm{cn}(\omega t)\,\mathrm{dn}(\omega t)}{1-\sin^2(\tfrac{1}{2}\phi_{\mathrm{i}})\,\mathrm{sn}(\omega t)}\end{aligned} \tag{3.5a}$$

where

$$A(T) = k\,\mathrm{cn}\,\alpha\,\mathrm{dn}\,\alpha = \frac{\sin(\tfrac{1}{2}\phi_{\mathrm{f}})[1-\sin^2(\tfrac{1}{2}\phi_{\mathrm{i}})\,\mathrm{sn}^2(\omega T)]-\sin(\tfrac{1}{2}\phi_{\mathrm{i}})\,\mathrm{cn}(\omega T)\,\mathrm{dn}(\omega T)}{\mathrm{sn}(\omega T)}. \tag{3.5b}$$

Notice that there are singularities in the solution due to the singularities of $A(T)$. One set of these singularities occurs at the zeros of the elliptic function $\mathrm{sn}(\omega T)$ at

$$\omega T = 2nK+2\mathrm{i}mK' \tag{3.6}$$

where m and n are integers and K and $\mathrm{i}K'$ are the real and imaginary quarter periods, respectively. These singularities correspond to the focal points suggested at the start of this subsection.

3.3. Evaluation of the WKB action

The starting point for evaluating the WKB action is the energy conservation equation. We note that the total energy E determines the value of the modulus k,

$$E = \tfrac{1}{2}\lambda p^2 + (2\omega^2/\lambda)\sin^2(\tfrac{1}{2}\phi) = 2(k\omega)^2/\lambda. \tag{3.7a}$$

Also, equivalently, if ϕ_0 is a turning point we have

$$k = \sin(\tfrac{1}{2}\phi_0). \tag{3.7b}$$

The energy equation (3.7a) can now be rewritten in terms of the velocity as

$$\dot{\phi}^2(t) = 4\omega^2[k^2 - \sin^2(\tfrac{1}{2}\phi)]. \tag{3.8}$$

Hence the expression for the time T evaluated along some path defined on a suitable complex Riemann surface for ϕ is

$$\omega T = \tfrac{1}{2}\int_{\phi_i}^{\phi_f} \mathrm{d}\phi[k^2 - \sin^2(\tfrac{1}{2}\phi)]^{-1/2}. \tag{3.9}$$

The branch points of the square root velocity factor occur at turning points, some of which are shown in figure 1. Figure 2 shows a two-sheeted Riemann surface for ϕ, where we have chosen to cut the surface between the turning points along the forbidden region. As discussed in § 2 it is convenient to choose the initial and final positions in the forbidden region as shown in figure 1. There is an ambiguity on which side of the cut to choose ϕ_i and ϕ_f and this results in spurious non-physical saddle points as discussed in § 2. Distinct paths will circulate the turning points tracing out very complicated curves. These paths will, nevertheless, be made up from arbitary multiples of pieces equivalent to the loops α and β shown in figure 2. The path α corresponds to a complete period of real oscillation, while the loop β represents a complete back

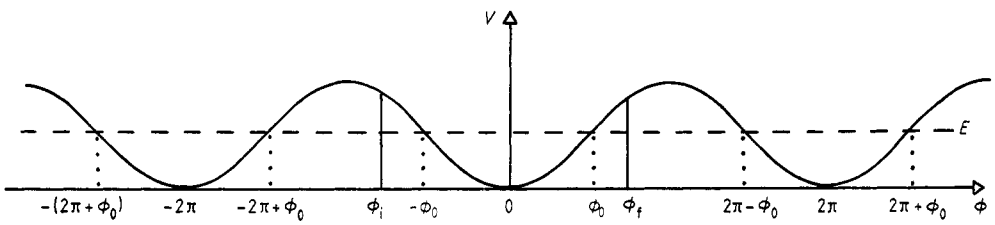

Figure 1. The periodic potential.

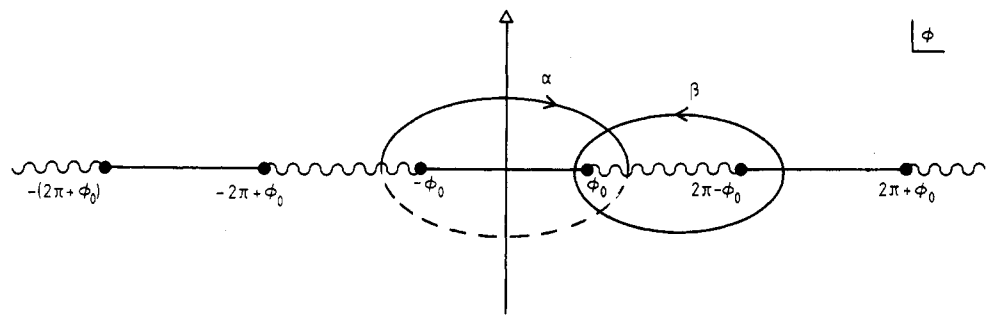

Figure 2. The Riemann surface for the variable ϕ, showing cuts as wavy lines between the turning points along the forbidden region.

and forth tunnelling through the forbiden region. The times for these loops are given by the full real and imaginary periods which are given by the integrals

$$\omega T_\alpha = \tfrac{1}{2}\int_\alpha \mathrm{d}\phi[k^2 - \sin^2(\tfrac{1}{2}\phi)]^{-1/2} = 4K \tag{3.10a}$$

$$\omega T_\beta = \tfrac{1}{2}\int_\beta \mathrm{d}\phi[k^2 - \sin^2(\tfrac{1}{2}\phi)]^{-1/2} = -4\mathrm{i}K'. \tag{3.10b}$$

The integrals in equation (3.9) are more easily identified as elliptic integrals in terms of a new variable ψ defined by

$$\sin(\tfrac{1}{2}\phi) = k \sin\psi \tag{3.11a}$$

$$p_\phi = (2\omega k/\lambda)\cos\psi. \tag{3.11b}$$

Figure 3 shows the new Riemann surface for ψ. Notice that when ψ is real, T is also real. The equation for the time now becomes

$$\omega T = \int_{\psi_i}^{\psi_f} \mathrm{d}\psi(1 - k^2\sin^2\psi)^{-1/2}. \tag{3.12}$$

In terms of the new variable the WKB action is

$$\begin{aligned} W_{\mathrm{cl}} &= \int_{\phi_i}^{\phi_f} p_\phi \,\mathrm{d}\phi \\ &= \frac{4\omega}{\lambda}\int_{\psi_i}^{\psi_f} \mathrm{d}\psi[(1 - k^2\sin^2\psi)^{1/2} - k'^2(1 - k^2\sin^2\psi)^{-1/2}] \end{aligned} \tag{3.13}$$

where k' is the complementary modulus given by $k'^2 = 1 - k^2$.

The most important quantities for determining the bound-state energies are the WKB action evaluated for the closed loop paths α and β, which from (3.13) can be shown to be

$$W_\alpha = (16\omega/\lambda)(E - k'^2 K) \equiv 2\hbar\omega_\alpha \tag{3.14a}$$

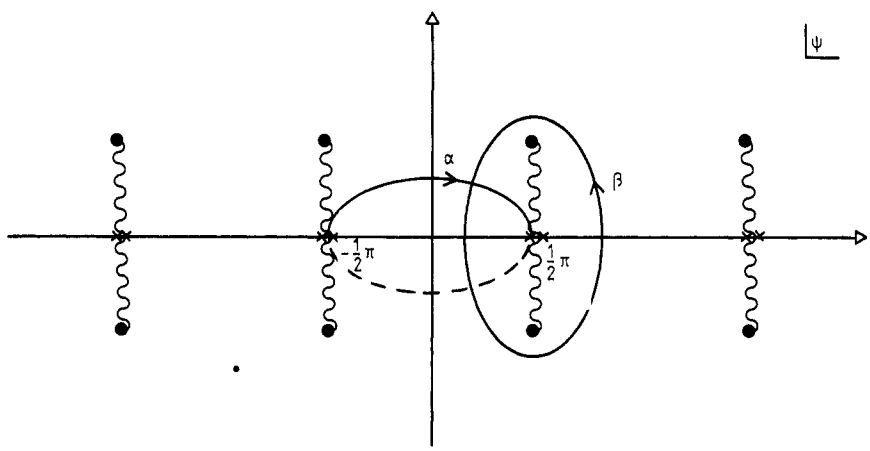

Figure 3. Riemann surface for the variable ψ. The turning points correspond to the junction of the cuts and the real axis. The broken curve represents the portion of the contour on the lower sheet.

and

$$W_\beta = (16i\omega/\lambda)(E' - k^2K') \equiv 2i\hbar\Delta \tag{3.14b}$$

where K and E are the complete elliptic integrals of the first and second kind; K' and E' have the modulus k replaced by the complementary modulus k'.

The physical path of minimum real and imaginary time is shown in figure 4. The time and action required in tunnelling from the initial position ϕ_i to the turning point L at $-\phi_0$ are denoted by $\omega T_i = -i\Omega_i$ and $W_i = i\hbar\Delta$. Similar notation with f replacing i is used for the right-hand tunnelling motion. The exact expressions can be evaluated but are not necessary for our results.

3.4. Classification of classical paths

Physically, the allowed motions are easy to identify. First, the paths fall into four categories depending on whether the motion starts or ends moving to the right or left. It is, however, more complicated to classify and count all the multiple tunnelling terms and this will be postponed until § 5. In the rest of this subsection we will relate these preliminary categories to the solutions and times derived earlier in this section.

We can now return to the solution (3.3) and observe that the initial condition (3.4*a*) can be satisfied by

$$\alpha_\pm = -K \pm i\Omega_i \tag{3.15}$$

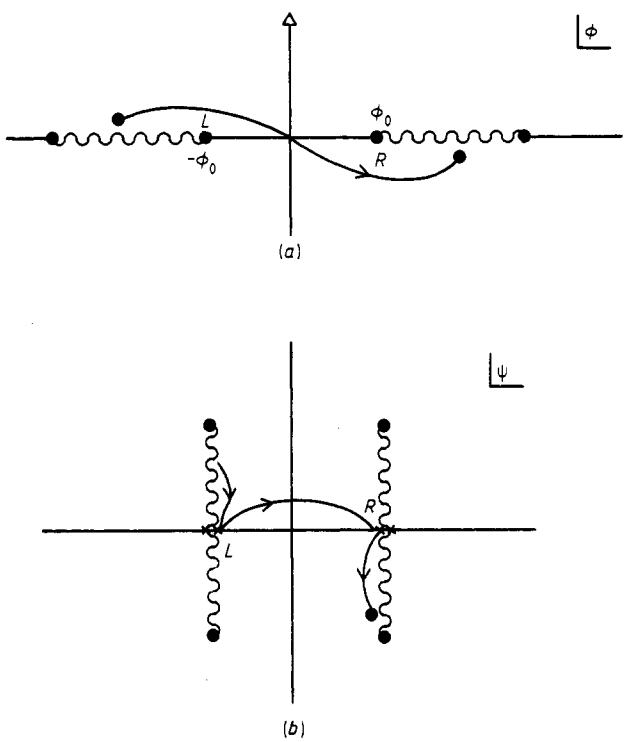

Figure 4. The path of minimum real and imaginary time (*a*) for the variable ϕ and (*b*) for the variable ψ.

(recall that ϕ_i is negative). Now as time develops the solution will pass through the final position ϕ_f at the saddle times T_s given by

$$\sin(\tfrac{1}{2}\phi_f) = k\,\mathrm{sn}(\omega T_s + \alpha). \tag{3.16}$$

This predicts the saddle times

$$\omega T_s = 2(2n+1)K + 2\mathrm{i}mK' - \mathrm{i}(\pm\Omega_i \pm \Omega_f). \tag{3.17}$$

Not all these saddles correspond to physical motions. Consider first the sequence of critical points

$$\omega T_I = 2(2n+1)K - \mathrm{i}(\Omega_i + \Omega_f) \qquad n = 0, 1, 2, \ldots. \tag{3.18}$$

The corresponding paths in the ψ plane for $n = 0$ and 1 are shown in figure 5. The ambiguity over which side of the cut to choose the initial and final angles ϕ_i and ϕ_f translates in the ψ plane into both ψ_i and its complex conjugate ψ_i^* satisfying the initial (and final) conditions. Consider path II shown in figure 6. It can be seen that the time elapsed is

$$\begin{aligned}\omega T_{II} &= -\mathrm{i}(K' - \Omega_i) - 3\mathrm{i}K' + 2K - 3\mathrm{i}\Omega_f \\ &= -\mathrm{i}(\Omega_f - \Omega_i) + 2K - 4\mathrm{i}K'.\end{aligned} \tag{3.19}$$

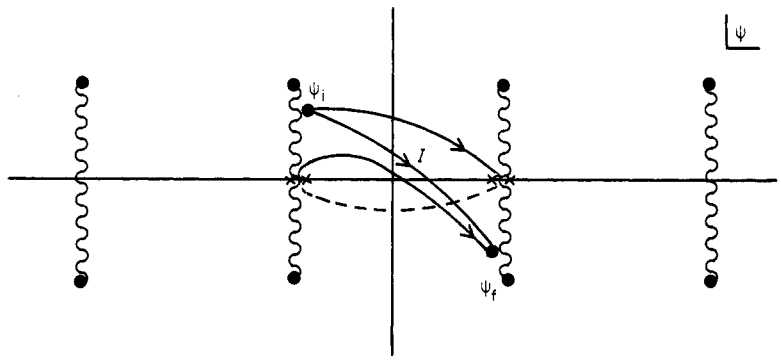

Figure 5. Two possible paths on the ψ Riemann surface which elapse minimum imaginary time. The longer path elapses an additional period of real time.

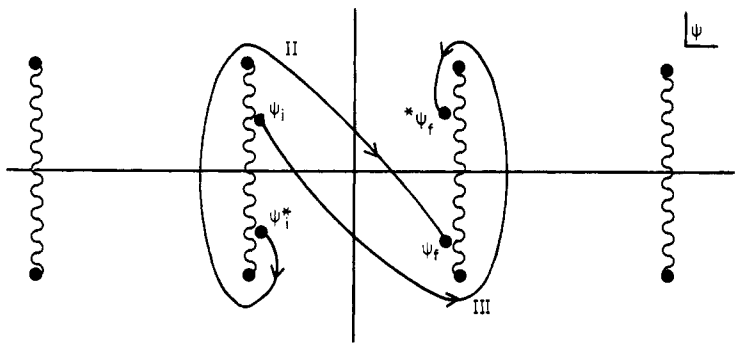

Figure 6. Two possible complex paths on the ψ Riemann surface.

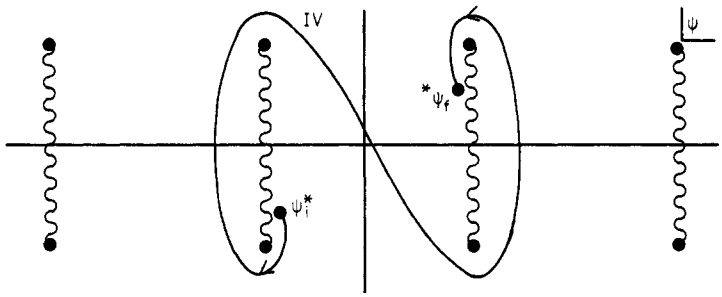

Figure 7. Another possible path on the ψ Riemann surface for which the elapsed real time is a minimum.

Path III shown in figure 6 is interpreted in a similar way and corresponds to an elapsed time

$$\omega T_{III} = i(\Omega_f - \Omega_i) + 2K - 4iK'. \tag{3.20}$$

Figure 7 shows another distinct physical path which requires a time

$$\omega T_{IV} = i(\Omega_f + \Omega_i) + 2K - 8iK'. \tag{3.21}$$

Paths I, II, III and IV are the four categories of path outlined at the start of this subsection. More complicated paths are built up from these by further circulation of the turning points and this is equivalent to adding any number of α and β loops.

4. Pendulum motion excluding tunnelling terms

The pendulum potential is like the harmonic oscillator but with less steep sides. This difference in shape causes the energy levels to shift down. In this section we concentrate on calculating the size of this shift. In this approximation, which neglects tunnelling, the classical paths are exactly the same as those for the harmonic oscillator. Consequently, the form of the energy Green function is also exactly the same. Because an extensive analysis of this is given in [4] we only briefly outline the method for deriving the energy Green function in these circumstances.

We consider paths of type I which begin and end on opposite sides of the potential. The saddle times are given by equation (3.18) in the previous section. These are displayed in figure 8 with a suitable contour through the saddles. From the basic formula (2.15) we have [4]

$$G_0^0(\phi_f, \phi_i; E) = \frac{i \exp[-(\Delta_i + \Delta_f)]}{\hbar(\dot{\phi}_i \dot{\phi}_f)^{1/2}} e^{i\omega_\alpha} \sum_{n=0}^{\infty} (-1)^n \exp(2i\omega_\alpha n) \tag{4.1}$$

where a minus sign is picked up from the square root velocity term on each complete α circuit, due to passing two turning points. Summing the geometric series and noting from figure 4

$$\dot{\phi}_i = 2\omega \exp(\tfrac{1}{2}i\pi)[\sin^2(\tfrac{1}{2}\phi_i) - k^2]^{1/2} \tag{4.2a}$$

$$\dot{\phi}_f = 2\omega \exp(\tfrac{1}{2}i\pi)[\sin^2(\tfrac{1}{2}\phi_f) - k^2]^{1/2} \tag{4.2b}$$

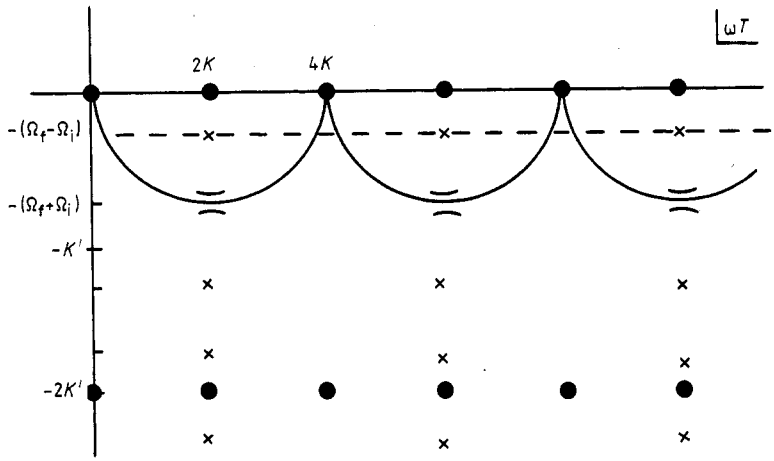

Figure 8. The complex time plane showing the steepest descent contour through the saddles from paths of type I. Singularities are represented by full circles and some other saddle-point positions are marked by crosses.

we obtain

$$G_0^0(\phi_f, \phi_i; E) = \frac{\exp[-(\Delta_i + \Delta_f)]}{2\omega\hbar\{[\sin^2(\frac{1}{2}\phi_f) - k^2][\sin^2(\frac{1}{2}\phi_i) - k^2]\}^{1/4}} \left(\frac{1}{2\cos\omega_\alpha}\right). \tag{4.3}$$

Poles in the propagator occur at the bound-state energy levels, which occur at the zeros of $\cos\omega_\alpha$. This gives the Bohr-Sommerfeld quantisation condition

$$\omega_\alpha/\pi = \tfrac{1}{2}(2n+1). \tag{4.4}$$

Notice that this gives levels with both positive and negative energies. This is of course wrong. As the energy moves towards the bottom of the potential well, the turning points approach and our simple formula breaks down. In this case we must make the replacement [4]

$$(1/2\cos\omega_\alpha) \to K(E) = \left(\frac{\omega_\alpha}{\pi e}\right)^{\omega_\alpha/\pi} \Gamma(\tfrac{1}{2} - \omega_\alpha/\pi) \frac{1}{(2\pi)^{1/2}}. \tag{4.5}$$

$K(E)$ has positive energy poles in the same positions as $(1/2\cos\omega_\alpha)$ but no negative energy poles. We note that the results so far presented are valid for any sufficiently smooth non-singular potential. Specialising in the pendulum and writing $m = k^2$ the quantisation condition gives

$$\begin{aligned}\lambda\hbar(2n+1)/8\omega &= 2(E - m_1 K)/\pi \qquad \text{with } m_1 = 1 - m \\ &= (\tfrac{1}{2}m)\{1 + (\tfrac{1}{2})^2(\tfrac{1}{2}m) + \left(\frac{1\times 3}{2\times 4}\right)^2 (\tfrac{1}{3}m^2) + \ldots \\ &\quad + [(1\times 3\times\ldots\times(2n+1))/(2\times 4\times\ldots\times 2n)]^2[m^n/(n+1)] + \ldots\}. \end{aligned} \tag{4.6}$$

Writing $\gamma = (2n+1)(\lambda\hbar/4\omega)$ we can invert the series to obtain the energy

$$\varepsilon_n^0 = 2\omega^2 m/\lambda = (2n+1)(\tfrac{1}{2}\hbar\omega)\left(1 - \frac{\gamma}{2^3} - \frac{\gamma^2}{2^6} - \frac{5\gamma^3}{2^{10}} - \frac{33\gamma^4}{2^{14}} - \frac{252\gamma^5}{2^{18}} + \ldots\right). \tag{4.7}$$

The first term is clearly the ordinary harmonic oscillator energy. The corrections correspond to the large-n limit of the exact asymptotic expansion in the region $E \ll 2\omega^2/\lambda$, i.e. $m \ll 1$ [13-15]. This is as we expect for a semiclassical method. Corrections arise from the approximate Feynman kernel (2.1). In this case approximation of (2.4) by steepest descent does not affect the position of poles of G (apart from excluding those of negative energy). However, in general this approximation will also make a contribution to the error.

We now consider paths which start and end on the same side of the potential. With the angle the same as previously this will occur for winding number $\nu = -1$ ($\phi_f^{-1} = \phi_f - 2\pi$). Figure 9 shows some of the simplest paths for this case. The saddle times are given by

$$\omega T_s = -i(\Omega_f - \Omega_i) - 2iK' + 4nK. \tag{4.8}$$

This sequence of saddles is shown in figure 10. The additional saddle drawn on the diagram corresponds to the direct passage from the initial angle ϕ_i to the final angle $(\phi_f - 2\pi)$. It is, however, excluded from this sum over saddles because the path approaches the final angle from the left. The first critical point we consider corresponds to a reflection in the forbidden region. Notice that the path through the critical points approaches this saddle by a descending ridge, at which it takes a 90° bend and proceeds along the steepest descent path to the next focal point (which corresponds to $-\phi_i - 2\pi$). Consequently, this saddle point is assigned a weight factor of $\frac{1}{2}$. This is a reflection of being precisely on a Stokes discontinuity where the form of the asymptotic expansion abruptly changes [12]. Following the paths shown in figure 11 we see that the square root velocity factors have opposite signs for the first and second terms. All subsequent

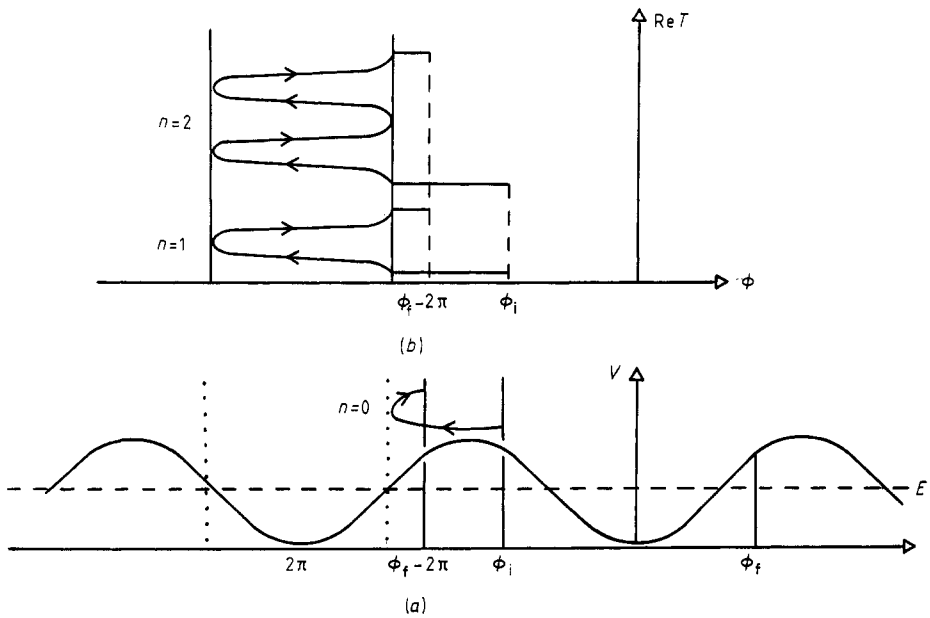

Figure 9. (*a*) The periodic potential with the simplest path of winding number −1, which never emerges from the forbidden region. (*b*) The elapsed real time for the paths of winding number −1 but with one and two bounces in the allowed region and the same imaginary time as in (*a*).

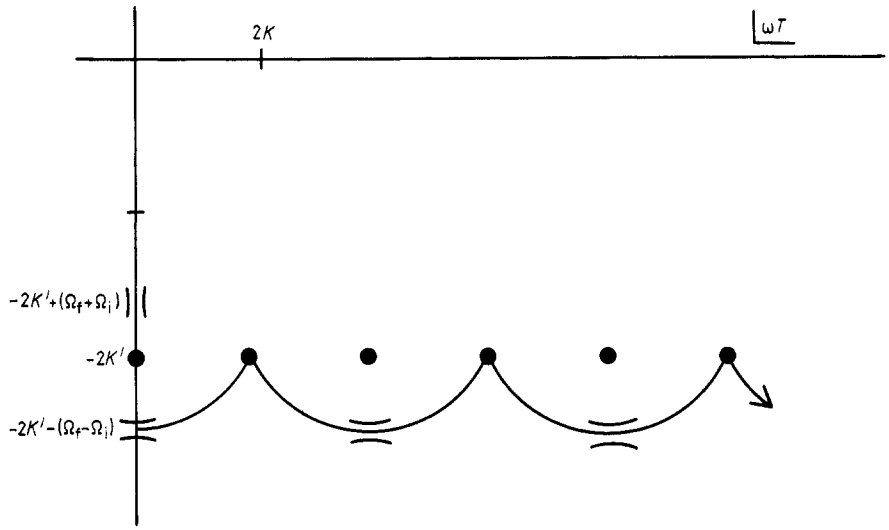

Figure 10. The relevant saddles and contour in the complex-time plane appropriate for winding number −1 and the sequence of paths indicated in figure 9.

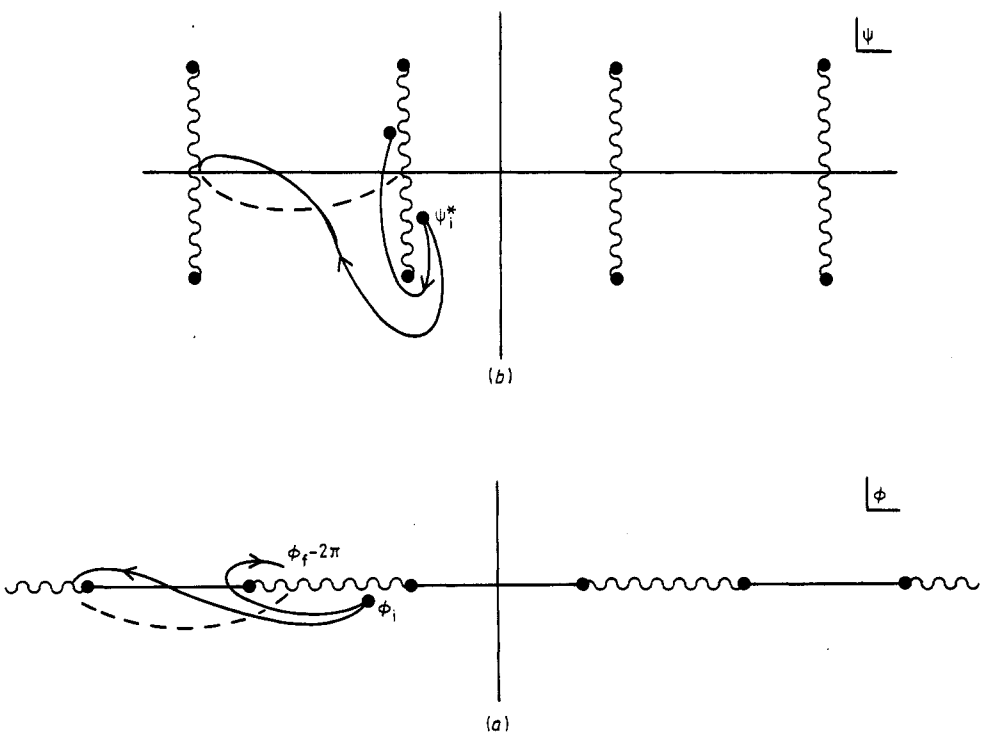

Figure 11. The two simplest paths of winding number −1 on the Riemann surface (*a*) for ϕ and (*b*) for ψ.

critical points contribute an additional minus sign for each full loop around the turning points [4]. Hence, we have for this sequence of saddles

$$G^0_{-1}(\phi_f, \phi_i; E) = \frac{\exp(-\Delta)\exp[-(\Delta_i+\Delta_f)]}{2\hbar\omega\{[\sin^2(\frac{1}{2}\phi_f)-k^2][\sin^2(\frac{1}{2}\phi_i)-k^2]\}^{1/4}}\left(\tfrac{1}{2}i + i\sum_{n=1}^{\infty}(-1)^n\exp(2i\omega_\alpha)\right)$$
$$= \frac{\exp(-\Delta)\exp[-(\Delta_i+\Delta_f)]}{2\hbar\omega\{[\sin^2(\frac{1}{2}\phi_f)-k^2][\sin^2(\frac{1}{2}\phi_i)-k^2]\}^{1/4}}\left(\frac{\sin\omega_\alpha}{2\cos\omega_\alpha}\right). \tag{4.9}$$

Observe that the pole positions are the same as the zero winding number case. We can now now make use of these two results to construct the full propagator including the effects of tunnelling.

5. Tunnelling and band energies

The essential difficulty in implementing our basic formula (2.15) is to enumerate all possible motions to be included in the sum. How this can be achieved is shown in the appendix. However, the approximation scheme we employ does not require the full result. We divide this section into subsections.. The first gives the calculation of the energy Green function. The next subsection gives the result for the energy bands together with the conditions for this to be valid. In the final subsection we give an interpretation of the approximations we make together with the wavefunctions.

5.1. The energy Green function

We begin by considering paths of zero winding number of type I. Figure 12 shows some representative paths classified by the number of complete back and forth transits through the forbidden region. Each of the partial motions pictured for the allowed regions stands for an infinite sum of paths. These sums were calculated in the previous section for the two different cases where the motion starts and finishes on the same or opposite side of the potential. Our approximation will neglect any difference between these two cases. Noting that each type of path occurs an even number of times and comparing equations (4.3) and (4.9) we see that this requires $\sin^2\omega_\alpha \approx 1$. In § 4, where tunnelling was ignored, this holds exactly at the energy levels. Provided tunnelling shifts the levels by exponentially small amounts this will be a good approximation (see the appendix for further justification). The physical consequences of this condition will be given in the next subsection.

Given this approximation we now need to calculate the weight factor corresponding to the number of different ways of obtaining terms with the same degree of suppression. This is shown explicitly for the first three cases in figure 12. The general case is calculated by representing each passage through the forbidden region as a step in a random walk. With a total of $2n$ steps, n to the right and n to the left, the total number of possibilities is

$$\frac{(2n)!}{(n!)^2} = \binom{2n}{n}. \tag{5.1}$$

Now formula (2.15) gives the partial propagator as the sum

$$G^1_0(\phi_f, \phi_i; E) = G^0_0(\phi_f, \phi_i; E)\sum_{n=0}^{\infty}\exp(-2n\Delta)\binom{2n}{n}\left(\frac{1}{2\cos\omega_\alpha}\right)^{2n}. \tag{5.2}$$

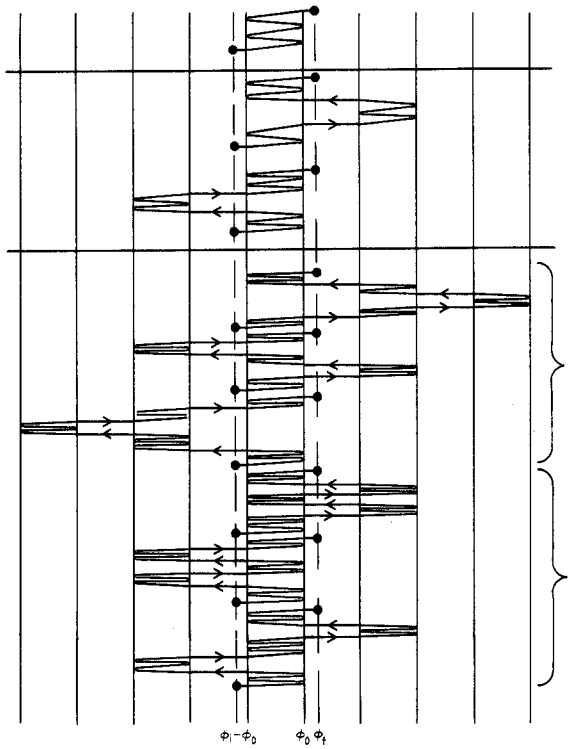

Figure 12. A sample of the classes of paths involving zero, one and two complete back and forth tunnellings through the forbidden region. A representative one or two back and forth bounces in each allowed region are shown, but we must remember that all possible numbers of bounces must be summed over. In the lower illustrations, paths whose sums are the same are grouped together.

Writing

$$x = e^{-\Delta}/\cos\omega_\alpha \tag{5.3}$$

and substituting the integral expression for $(2n)!$ we obtain

$$\begin{aligned} G_0^1(\phi_f, \phi_i; E) &= G_0^0(\phi_f, \phi_i; E)\int_0^\infty e^{-t}\sum_{n=0}^{\infty}\frac{(\frac{1}{2}xt)^{2n}}{(n!)^2}\,dt \\ &= G_0^0(\phi_f, \phi_i; E)\int_0^\infty e^{-t} I_0(xt)\,dt. \end{aligned} \tag{5.4}$$

This integral is easily evaluated; however, it is already in a convenient form for our purposes as will be shown presently.

In the same approximation scheme we will now consider the expression for the terms in the propagator corresponding to non-zero winding number. For positive winding number ν the final angle is $\phi_f^\nu = 2\pi\nu + \phi_f$. For $2n$ transits through the forbidden region, in addition to the ν for the winding number, we have $n+\nu$ steps to the right and n steps to the left. The total number of possibilities is therefore

$$\binom{2n+\nu}{n} = \binom{2n+\nu}{n+\nu}. \tag{5.5}$$

In the case of negative winding number $\nu = -\mu$ we have exactly the same situation with left and right reversed. The total number of possibilities is

$$\binom{2n+\mu}{n}. \tag{5.6}$$

Hence we can now write the propagator for winding number ν, again only for paths of type I, as

$$\begin{aligned} G^{\mathrm{I}}_{\nu}(\phi_{\mathrm{f}}, \phi_{\mathrm{i}}; E) &= G^{0}_{0}(\phi_{\mathrm{f}}, \phi_{\mathrm{i}}; E) \sum_{n=0}^{\infty} (\tfrac{1}{2}x)^{2n+|\nu|} \binom{2n+|\nu|}{n} \\ &= G^{0}_{0}(\phi_{\mathrm{f}}, \phi_{\mathrm{i}}; E) \int_{0}^{\infty} \mathrm{e}^{-t} I_{\nu}(xt)\, \mathrm{d}t. \end{aligned} \tag{5.7}$$

The Feynman path integral demands that we sum over all possible paths between the initial and final angles. Recall that, when interpreted as a pendulum confined to a circle, the paths fall into disconnected classes represented by the winding number. An arbitary phase factor will therefore arise for each disconnected class of paths in the Feynman sum over histories. However, the symmetry of the system reduces this arbitariness to a single phase factor δ between successive winding number contributions [2]. This idea is crucial in obtaining a band of levels. The demonstration of this result in [2] hinges on the fact that the proof that the path integral satisfies Schrödinger's equation is a local one. Hence the propagator for each winding number should individually satisfy the Schrödinger equation. This forms the path integral version of Bloch's theorem. In fact, for Bloch waves, on translating the wavefunction from one lattice site to the next, the phase should advance by $2\pi ka$, where k is the wavenumber and a the lattice spacing. This factor of $2\pi ka$ is identified with the phase δ. We can now write the full propagator as

$$\begin{aligned} G^{\mathrm{I}}(\phi_{\mathrm{f}}, \phi_{\mathrm{i}}; E) &= \sum_{\nu=-\infty}^{+\infty} \mathrm{e}^{\mathrm{i}\nu\delta} G^{\mathrm{I}}_{\nu}(\phi_{\mathrm{f}}, \phi_{\mathrm{i}}; E) \\ &= G^{0}_{0}(\phi_{\mathrm{f}}, \phi_{\mathrm{i}}; E) \sum_{\nu=-\infty}^{+\infty} \mathrm{e}^{\mathrm{i}\nu\delta} \int_{0}^{\infty} \mathrm{e}^{-t} I_{\nu}(xt)\, \mathrm{d}t. \end{aligned} \tag{5.8}$$

Now using the generating function identity for Bessel functions

$$\sum_{\nu=-\infty}^{+\infty} y^{\nu} I_{\nu}(z) = \exp[\tfrac{1}{2}z(y+1/y)] \tag{5.9}$$

we obtain the final result for the energy Green function

$$\begin{aligned} G^{\mathrm{I}}(\phi_{\mathrm{f}}, \phi_{\mathrm{i}}; E) &= G^{0}_{0}(\phi_{\mathrm{f}}, \phi_{\mathrm{i}}; E) \int_{0}^{\infty} \exp\{-t[1-(\cos\delta)x]\}\, \mathrm{d}t \\ &= \frac{G^{0}_{0}(\phi_{\mathrm{f}}, \phi_{\mathrm{i}}; E)}{1-(\cos\delta)x}. \end{aligned} \tag{5.10}$$

Substituting for G^{0}_{0} and x, expression (5.10) becomes

$$G^{\mathrm{I}}(\phi_{\mathrm{f}}, \phi_{\mathrm{i}}; E) = \frac{\exp[-(\Delta_{\mathrm{i}}+\Delta_{\mathrm{f}})]}{2\hbar\omega\{[\sin^{2}(\frac{1}{2}\phi_{\mathrm{f}}) - k^{2}][\sin^{2}(\frac{1}{2}\phi_{\mathrm{i}}) - k^{2}]\}^{1/4}} \frac{1}{[\cos\omega_{\alpha} - \cos\delta\exp(-\Delta)]}. \tag{5.11}$$

5.2. Energy levels for the pendulum

The energy levels are given by the poles in (5.11) which occur when

$$\cos \omega_\alpha = \cos \delta \exp(-\Delta). \tag{5.12}$$

It is important to realise that the derivation of this result was independent of any specific properties of the pendulum potential. It will apply to any sufficiently smooth bounded periodic potential.

We will now present the general result for the bandwidth. Since we wish to have results valid near the bottom of the potential well, where the turning points merge, we make the replacement given by equation (4.5). It is then possible to see that the bandwidth is given by

$$2\hbar\omega\left(\frac{2}{\pi}\right)^{1/2}\left(\frac{n+\frac{1}{2}}{e}\right)^{n+1/2}\frac{\exp(-\Delta)}{n!}. \tag{5.13a}$$

The frequency for the approximate oscillator at the bottom of the potential well is ω and Δ is a more general integral around the turning points in the forbidden region

$$\Delta = \frac{1}{2i\hbar}\oint_\beta p \, d\phi \tag{5.13b}$$

where p is the generalised momentum. Recall that at the beginning of § 5.1 we made the approximation that the tunnelling factor Δ was large. Consequently, the tunnelling probability is small and so we require either tight binding or widely separated potential wells. Result (5.13) is identical to that derived by Harrell [16] from a rigorous analysis of the differential equation.

We now return to the specific case of the pendulum potential and recall from (3.14*b*) that

$$\Delta = \frac{8\omega}{\lambda\hbar}(E' - k^2K'). \tag{5.14}$$

Now using the expansions for the elliptic function we have the explicit expression

$$\begin{aligned} E' - k^2K' = {} & 1 + \tfrac{1}{4}m(\ln m - 4\ln 2 - 1) + \tfrac{1}{32}m^2(\ln m - 4\ln 2 + \tfrac{3}{2}) \\ & + \tfrac{1}{2}m\sum_{n=2}^{\infty}\left(\frac{1\times 3\times\ldots\times(2n-1)}{2^n n!}\right)^2\frac{m^n}{2(n+1)} \\ & \times[\ln m - 4\ln 2 + 4(1 - \tfrac{1}{2} + \tfrac{1}{3}\ldots - 1/2n) - 1/(n+1)] \end{aligned} \tag{5.15}$$

Substituting for the value of m from equation (4.7) which neglects tunnelling we obtain

$$E' - k^2K' = 1 - \tfrac{1}{4}\gamma + \tfrac{5}{64}\gamma^2 + \ldots + \tfrac{1}{4}\gamma(1 + O(\gamma^2))\ln\gamma(1 - \tfrac{1}{8}\gamma) - \gamma(1 + O(\gamma^2))\ln 2 + \ldots. \tag{5.16}$$

As we wish our results to be valid near the bottom of the potential well we again make the replacement given by equation (4.5). Hence we obtain the band of levels

$$\begin{aligned} \varepsilon_n = {} & \varepsilon_n^0 + (-1)^n\hbar\omega\frac{\cos\delta}{n!}2^{2(2n+1)}\left(\frac{2}{\pi}\right)^{1/2}\left(\frac{2\omega}{\lambda\hbar}\right)^{n+1/2} \\ & \times\exp(-8\omega/\lambda\hbar)\left[1 - \tfrac{3}{32}(2n+1)^2\left(\frac{\lambda\hbar}{4\omega}\right) - \ldots\right]. \end{aligned} \tag{5.17}$$

This agrees with the results obtained by Goldstien [14], Dingle and Müller [15] and the bandwidth presented by Stone and Reeve [13]. Also, if we specialise in the

ground-state result, we obtain exactly the instanton result, plus a correction to it [7, 17]. The correction is of the correct sign but somewhat smaller than the actual value [14, 15, 17]. This is quite reasonable as we only expect the method to give the corrections in the semiclassical large-n limit. We also note that, specialising in the case when the Bloch phase $\delta = 0$, we obtain the result for the simple pendulum.

Remember that at the beginning of this section we made the approximation that the tunnelling factor Δ was large. This was because we require $\cos \omega_\alpha$ to be small, an assumption that is now seen to be consistent with (5.12). Notice that the scale factor multiplying the elliptic functions in (5.14) is $8\omega/\lambda\hbar$. Thus, examining equation (5.15), we see that provided m is small $\Delta \gg 1$ implies $8\omega/\lambda\hbar \gg 1$. At the top of the potential well, where this condition breaks down ($m = 1$ and $\Delta = 0$), we also note that the saddle-point method fails because the turning points coalesce.

We now summarise our results and their limitations. Observe that other sufficiently smooth bounded periodic potentials are solved by equations (4.4) and (5.12), provided the expressions ω_α and Δ of (3.14a) and (3.14b) are replaced by the corresponding more general action integrals. We have shown that equation (5.17) together with equation (4.7) give a good approximation to the bound-state energies of the pendulum provided

$$(8\omega/\lambda\hbar) \gg 1 \qquad \text{and} \qquad m = (E\lambda/2\omega^2) \ll 1.$$

Equations (4.7) and (5.17) provide good approximations given the above criteria, but we also note that for small n other corrections become important. For each order in the $(\lambda\hbar/8\omega)$ series, additional terms in lower powers of n will occur. A measure of the size of these corrections to (5.17) is given by the discussion following equation (5.17). For the corrections to equation (4.7) for small n we refer the reader to [13].

5.3. Interpretation of the results

We now find the wavefunctions in order to provide a basis for comparing our results with other methods. To achieve this we must complete the calculation by including the contributions from paths of types II, III and IV. This is straightforward. Calculations along the lines already given for paths of type I give

$$G^{\mathrm{II}}(\phi_\mathrm{f}, \phi_\mathrm{i}; E) = \frac{\exp[-(\Delta - \Delta_\mathrm{i})]\exp(-\Delta_\mathrm{f})}{2\hbar\omega\{[\sin^2(\tfrac{1}{2}\phi_\mathrm{f}) - k^2][\sin^2(\tfrac{1}{2}\phi_\mathrm{i}) - k^2]\}^{1/4}} \frac{\exp(\mathrm{i}\delta)}{[\cos\omega_\alpha - \cos\delta\exp(-\Delta)]} \tag{5.18a}$$

$$G^{\mathrm{III}}(\phi_\mathrm{f}, \phi_\mathrm{i}; E) = \frac{\exp[-(\Delta - \Delta_\mathrm{f})]\exp(-\Delta_\mathrm{i})}{2\hbar\omega\{[\sin^2(\tfrac{1}{2}\phi_\mathrm{f}) - k^2][\sin^2(\tfrac{1}{2}\phi_\mathrm{i}) - k^2]\}^{1/4}} \frac{\exp(\mathrm{i}\delta)}{[\cos\omega_\alpha - \cos\delta\exp(-\Delta)]} \tag{5.18b}$$

$$G^{\mathrm{IV}}(\phi_\mathrm{f}, \phi_\mathrm{i}; E) = \frac{\exp[-(\Delta - \Delta_\mathrm{i})]\exp[-(\Delta - \Delta_\mathrm{f})]}{2\hbar\omega\{[\sin^2(\tfrac{1}{2}\phi_\mathrm{f}) - k^2][\sin^2(\tfrac{1}{2}\phi_\mathrm{i}) - k^2]\}^{1/4}} \frac{\exp(2\mathrm{i}\delta)}{[\cos\omega_\alpha - \cos\delta\exp(-\Delta)]}. \tag{5.18c}$$

The full propagator can then be written as

$$\begin{aligned} G(\phi_\mathrm{f}, \phi_\mathrm{i}; E) &= G^{\mathrm{I}} + G^{\mathrm{II}} + G^{\mathrm{III}} + G^{\mathrm{IV}} \\ &= \frac{\exp(-\Delta)\{\exp(\tfrac{1}{2}\Delta - \Delta_\mathrm{f}) + \exp(\mathrm{i}\delta)\exp[-(\tfrac{1}{2}\Delta - \Delta_\mathrm{f})]\} \times \{\exp(\tfrac{1}{2}\Delta - \Delta_\mathrm{i}) + \exp(\mathrm{i}\delta)\exp[-(\tfrac{1}{2}\Delta - \Delta_\mathrm{i})]\}}{2\hbar\omega\{[\sin^2(\tfrac{1}{2}\phi_\mathrm{f}) - k^2][\sin^2(\tfrac{1}{2}\phi_\mathrm{i}) - k^2]\}^{1/4}[\cos\omega_\alpha - \cos\delta\exp(-\Delta)]} \\ &\equiv \sum_n \frac{\psi_n(\phi_\mathrm{f})\psi_n^*(\phi_\mathrm{i})}{E - E_n}. \end{aligned} \tag{5.19}$$

Hence we obtain the WKB wavefunctions in the forbidden region to be

$$\psi_n(\phi_f) = \frac{\exp(-\frac{1}{2}\Delta)\{\exp[(\frac{1}{2}\Delta - \Delta_f)] + \exp(i\delta)\exp[-(\frac{1}{2}\Delta - \Delta_f)]\}}{(2\pi)^{1/2}[\sin^2(\frac{1}{2}\phi_f) - k^2]^{1/4}}\Bigg|_{E=E_n}. \tag{5.20}$$

These results can be compared with the approximate wavefunctions given in [14]. The first term can be interpreted as a decreasing wave coming from the left while the second term is a decreasing wave coming from the right with an arbitary phase difference between them. The denominator contains the usual WKB velocity factor. These results can also be interpreted in terms of the Bloch wavefunctions of the tight binding approximation [18]. The first term roughly corresponds to a 'harmonic oscillator type orbital' centred on $\phi = 0$, while the second term corresponds to a similar nearest-neighbour 'orbital' centred on $\phi = 2\pi$, together with its Bloch phase. All the other terms have been neglected in the approximation because the tunnelling factor is much larger than one. This explains why the expression for the energy only contains terms in $\cos\delta$. If we included more than nearest-neighbour orbitals, the expression for the energy band would contain higher Fourier components. These will become more important close to the top of the potential well.

6. Discussion and conclusions

The classical path method has been shown to provide an effective and physically clear method of obtaining the band structure for the periodic potential, provided the energy is sufficiently below the top of the potential ($E = 2\omega^2/\lambda$). This limitation is by no means intrinsic to the method. However, in this case it is rather difficult to extend the method outside this region. (It is even quite difficult for the quadratic barrier [4]. Also, see [8] for the result in this region.) The aim of this paper has been to clearly display the semiclassical aspects of the result in the context of the path integral.

The instanton approach is also a path integral method for obtaining these results for the ground state only. This method concentrates on a special subset of classical solutions, the zero-energy solutions which tunnel from the bottom of one well to a neighbouring one. The Euclidean time Feynman propagator, K, for this solution now forms the basis of the approximation. Individual instantons (and anti-instantons) are viewed in the large-time limit as well localised objects. Now, other approximate solutions to the classical equations of motion consist of widely separated strings of instantons and anti-instantons. This construction is very similar to the path decomposition and sum presented in § 5.1. However, there are some important differences. In the instanton approach the allowed energies E_n are found from the large Euclidean time $\tau = iT$ behaviour of the Feynman kernel [7, 19]. For the periodic potential this is

$$\sum_{n=-\infty}^{+\infty} \exp(in\delta)\,\mathrm{Tr}\,K_n = \sum_{-\infty}^{+\infty} \exp(in\delta)\int d\phi_i\, K_n(\phi_f = \phi_i, \phi_i; -i\tau)$$
$$\equiv \sum_n \exp(-E_n(\delta)\tau/\hbar)$$

where K_n is the Feynman kernel for winding number n. The non-Gaussian integration over ϕ_i is done by replacing it by an integral over collective coordinates. We note that the classical path method avoids this step because the energy levels are obtained from the poles of the energy propagator.

Also, the instanton technique neglects any possible interaction between instantons, whereas the classical path approach includes all possible interactions. Zinn-Justin (19) has shown how to incorporate some instanton interactions. This modification of the instanton method gives results for the higher energy levels identical to formula (5.17). However, near the top of the potential well, naive considerations would anticipate that the instantons would disappear or become irrelevant, while the classical path method remains valid. Unfortunately, the approximation that the tunnelling factor Δ be large excludes this region.

Lowe and Stone [17] have obtained the second term in the asymptotic expansion for the ground-state bandwidth, from a 'two-loop' calculation about the instanton (without any instanton interaction). As noted earlier, our results (5.17) include a similar but smaller correction. To obtain improved results the classical path method must be extended beyond a leading-order asymptotic expansion.

Instantons have become of special interest in recent years because of their application to field theory [7, 11]. The classical path method generalises this approach and is in many ways simpler. However, the attractive feature of the instanton approach has been its application to field theory. Here attention is focused on instantons, which are finite action solutions to the Euclidean equations of motion. (This corresponds to restricting attention to zero energy for quantum mechanics.) The classical path method suggests that interest is widened to look for solutions of the field equations which have finite action in finite 4-volume.

Appendix. Exact expression for zero winding number kernel

Figure 12 shows the simplest paths of type I. Recall, from § 4, that the sum of real bounces from opposite sides of the potential give a contribution to the energy Green function of $(1/2 \cos \omega_\alpha)$. In contrast, those paths starting and ending on the same side of the potential give $(\sin \omega_\alpha/2 \cos \omega_\alpha)$. We require to make a systematic expansion in terms of the number of transits through the forbidden region. Figure 13 gives a diagram for this, with $2n$ full passages through the forbidden region and $2m$ changes in direction. Obviously, there must be at least one change in direction (if $n \neq 0$) and a maximum of n. For the right motion there is a total of $(n+1)$ possible links (i.e. successive right motion or a gap region of left motion) and m gaps. Thus the number of possible combinations is $\binom{n+1}{m}$.

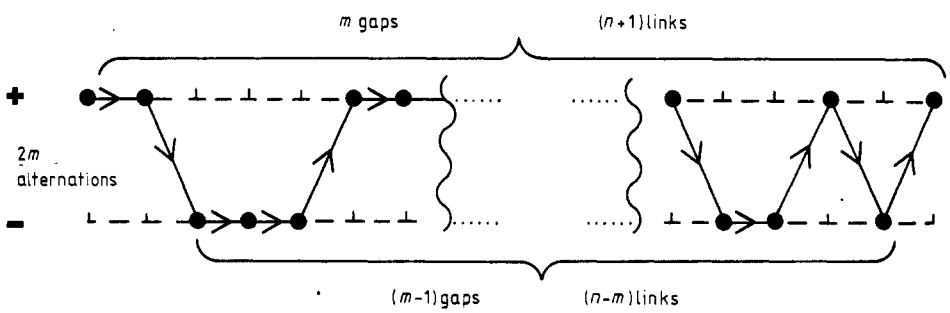

Figure 13. A diagram illustrating an example of paths with $2n$ transits through the forbidden region with $2m$ changes in direction. Each spot on the top line represents a step to the right, while a spot on the bottom line corresponds to a leftwards step. The start and end positions also correspond to a spot on the top line.

In the same way, for left motion there are $(n-1)$ links and $(m-1)$ gaps, giving $\binom{n-1}{m-1} = \binom{n-1}{n-m}$ combinations. Thus, the total number of possibilities is $\binom{n+1}{m}\binom{n-1}{n-m}$.

We note the important identity

$$\sum_{m=1}^{n} \binom{n+1}{m}\binom{n-1}{n-m} = \binom{2n}{n}.$$

The right-hand side represents the total number of independent ways of making $2n$ transits through the forbidden region, as shown in § 5.

The complete propagator for winding number zero and paths of type I is therefore

$$G_0^1(\phi_f, \phi_i; E) = G_0^0(\phi_f, \phi_i; E)\left\{1 + \sum_{n=1}^{\infty} \exp(-2n\Delta) \times \left[\sum_{m=1}^{n} \binom{n+1}{m}\binom{n-1}{n-m}\left(\frac{\sin\omega_\alpha}{2\cos\omega_\alpha}\right)^{2m}\left(\frac{1}{2\cos\omega_\alpha}\right)^{2(n-m)}\right]\right\} \tag{A1}$$

where G_0^0 is given by equation (4.3). Rewriting the expression in square brackets as

$$S_n = \sum_{m=1}^{n} \binom{n+1}{m}\left(\frac{\sin\omega_\alpha}{2\cos\omega_\alpha}\right)^{2m}\left[\sum_{k=0}^{n-1}\binom{n-1}{k}\left(\frac{1}{2\cos\omega_\alpha}\right)^{2k}\delta_{n-m-k}\right] \tag{A2}$$

facilitates the summation over m. This is achieved by writing the Krönecker delta function as

$$\delta_{n-m-k} = \frac{1}{2\pi}\int_{-\pi}^{+\pi} d\theta \exp[i\theta(n-m-k)]. \tag{A3}$$

Extending the summation ranges by making use of the delta function we obtain

$$S_n = \frac{1}{2\pi}\int_{-\pi}^{+\pi} d\theta \exp(in\theta)\sum_{m=0}^{n+1}\binom{n+1}{m}\left(\frac{\sin^2\omega_\alpha \exp(i\theta)}{4\cos^2\omega_\alpha}\right)^m\left[\sum_{k=0}^{n-1}\binom{n-1}{k}\left(\frac{\exp(i\theta)}{4\cos^2\omega_\alpha}\right)^k\right]. \tag{A4}$$

Writing $z = e^{i\theta}$ we can express the result as either a contour integral about the unit circle or an n-fold derivative,

$$S_n = \frac{1}{2\pi i}\oint dz \frac{(z+1/4\cos^2\omega_\alpha)^{n-1}(z+\sin^2\omega_\alpha/4\cos^2\omega_\alpha)^{n+1}}{z^{n+1}} \tag{A5a}$$

$$= \frac{1}{n!}\frac{d^n}{dz^n}\left[\left(z+\frac{1}{4\cos^2\omega_\alpha}\right)^{n-1}\left(z+\frac{\sin^2\omega_\alpha}{4\cos^2\omega_\alpha}\right)^{n+1}\right]\Bigg|_{z=0}. \tag{A5b}$$

The summation over n is now difficult without some simplification. The approximation $\cos\omega_\alpha \approx 0$ considered in § 5 suggests that we write

$$\frac{\sin^2\omega_\alpha}{4\cos^2\omega_\alpha} = \left(\frac{1}{2\cos\omega_\alpha}\right)^2 - \frac{1}{4}. \tag{A6}$$

Now the first term in (A6) is much the largest in the approximation regime we are considering. This suggests the expansion

$$S_n = \frac{1}{n!}\frac{d^n}{dz^n}\left[z+\left(\frac{1}{2\cos\omega_\alpha}\right)^2\right]^{2n}\left\{1-\frac{1}{4[z+(1/2\cos\omega_\alpha)^2]}\right)^{n+1}\Bigg|_{z=0}$$

$$= \binom{2n}{n}\left(\frac{1}{2\cos\omega_\alpha}\right)^{2n} - \left(\frac{n+1}{4}\right)\binom{2n-1}{n}\left(\frac{1}{2\cos\omega_\alpha}\right)^{2(n-1)} + \ldots. \tag{A7}$$

The first term is the approximation considered in § 5. Substituting the approximate solution (5.12) into this expression we see that the neglected term is smaller by a factor $e^{-2\Delta}$. This justifies the simplifications made in § 5.

References

[1] Berry M V and Mount K E 1972 *Rep. Prog. Phys.* **35** 315
[2] Schulman L S 1981 *Techniques and Applications of Path Integration* (New York: Wiley)
[3] Gutzwiller M P 1967 *J. Math. Phys.* **8** 1979; 1969 *J. Math. Phys.* **10** 1004; 1970 *J. Math. Phys.* **11** 1791; 1971 *J. Math. Phys.* **12** 343
[4] Carlitz R N and Nicole D A 1985 *Ann. Phys., NY* **164** 411
[5] McLaughlin D W 1972 *J. Math. Phys.* **13** 1099
[6] Carlitz R N 1984 *Pittsburgh preprint, PITT-19-84*
[7] Coleman S 1977 *The Whys of Subnuclear Physics* (*Erice Lectures*) ed A Zichichi (New York: Plenum) p 805
[8] Millard P A 1985 *Nucl. Phys.* B **259** 266
[9] Fröman N 1966 *Ark. Fys.* **32** 541; 1974 *Ann. Phys., NY* **83** 451; 1979 *J. Phys. A: Math. Gen.* **12** 2355
[10] Fröman N and Fröman P O 1974 *Ann. Phys., NY* **83** 103; 1974 *Nuovo Cimento* B **20** 121
[11] Dashen R F, Hasslacher B and Neveu A 1974 *Phys. Rev.* D **10** 4114
[12] Dingle R B 1973 *Asymptotic Expansions: Their Derivation and Interpretation* (New York: Academic)
[13] Stone M and Reeve J 1978 *Phys. Rev.* D **18** 4746
[14] Goldstien S 1929 *Proc. R. Soc. Edin.* **46** 210
[15] Dingle R B and Müller H J W 1962 *J. Rein Ang. Math.* **211** 26
[16] Harrell E M 1979 *Ann. Phys., NY* **119** 351
[17] Lowe M and Stone M 1978 *Nucl. Phys.* B **136** 177
[18] Ziman J M 1969 *Principles of the Theory of Solids* (Cambridge: Cambridge University Press)
[19] Zinn-Justin J 1981 *Nucl. Phys.* B **192** 125; 1983 *Nucl. Phys.* B **218** 333; 1984 *Recent Advances in Field Theory and Statistical Mechanics* (*Les Houches Lectures, 1982)* ed J B Zuter and R Stora (Amsterdam: Elsevier)